01 Jan 2017

Development Of Structural-functional Integrated Energy Storage Concrete With Innovative Macro-encapsulated PCM By Hollow Steel Ball

Hongzhi Cui

Waiching Tang

Qinghua Qin

Feng Xing

et. al. For a complete list of authors, see https://scholarsmine.mst.edu/civarc_enveng_facwork/2538

Recommended Citation

H. Cui et al., "Development Of Structural-functional Integrated Energy Storage Concrete With Innovative Macro-encapsulated PCM By Hollow Steel Ball," *Applied Energy*, vol. 185, pp. 107 - 118, Elsevier, Jan 2017. The definitive version is available at https://doi.org/10.1016/j.apenergy.2016.10.072

Applied Energy 185 (2017) 107–118

Contents lists available at ScienceDirect

Applied Energy

journal homepage: www.elsevier.com/locate/apenergy

Development of structural-functional integrated energy storage concrete with innovative macro-encapsulated PCM by hollow steel ball

Hongzhi Cui [a], Waiching Tang [b], Qinghua Qin [c], Feng Xing [a,*], Wenyu Liao [a], Haibo Wen [a]

[a] Guangdong Provincial Key Laboratory of Durability for Marine Civil Engineering, College of Civil Engineering, Shenzhen University, Shenzhen 518060, China
[b] School of Architecture and Built Environment, the University of Newcastle, Callaghan, NSW 2308, Australia
[c] Research School of Engineering, Australian National University, Canberra, ACT 2601, Australia

HIGHLIGHTS

- An innovative macro-encapsulation of PCM using HSB was developed.
- Macro-encapsulated PCM-HSB-c has high latent heat storage capacity (153.1 J/g).
- PCM-HSB-c concretes with structural and thermostatic properties were produced and demonstrated.
- Effect of thermal cycles on properties of the PCM concretes was investigated.
- Thermal performances of the PCM concretes were estimated by the rate of temperature decrease.

ARTICLE INFO

Article history:
Received 7 September 2016
Received in revised form 7 October 2016
Accepted 23 October 2016
Available online 7 November 2016

Keywords:
Macro-encapsulated phase change material
Hollow steel ball
Performance improvement
Elevated temperature test
Thermal performance
Thermal energy storage capacity

ABSTRACT

Phase change materials (PCMs) have great potential for applications in energy efficient buildings. In this study, an innovative method of macro-encapsulation of PCM using hollow steel balls (HSB) was developed and the thermal and mechanical performance of PCM-HSB concrete was examined. The macro-encapsulation system (PCM-HSB) was attached with a metal clamp (c) for better mechanical interlocking with the mortar matrix. The latent heat of PCM-HSB-c that can be acquired is approximately 153.1 J/g, which can be considered to rank highly among PCM composites. According to the self-designed thermal performance evaluation, the PCM–HSB-c concrete panel is capable of reducing and deferring the peak indoor temperature. The indoor temperature of the room model using PCM-HSB-c panels was significantly lower than the ones with normal concrete panels by a range of 3–6%. Furthermore, the test room using a higher PCM-HSB-c content demonstrated a greater ability to maintain a lower indoor room temperature for a longer period of time during heating cycles. In consideration of the mechanical properties, thermal performance and other aspects of cost factors, 50% and 75% PCM-HSB-c replacement levels are recommended in producing concrete.

1. Instruction

Rapidly growing world energy consumption has led to several serious problems, for example fossil fuel depletion, environmental pollution and increasing level of CO_2 emission [1,2]. The U.S. Energy Information Administration recently predicted that world energy consumption would grow by 48% between 2012 and 2040 [3]. Therefore, it is imperative to reduce the consumption of fossil energy in the world. Declines in fossil energy consumption and an increased proportion of renewable energy among energy consumption tend to be rooted in the adoption of more energy-efficient technologies [4–7]. In 2014 an estimated USD 90 billion (±10%) was invested to the energy efficiency of buildings. This is projected to increase to over USD 125 billion by 2020, driven by expanding environmentally friendly and efficiency-targeted policies [8]. Undoubtedly, building energy efficiency has become a principal objective for energy policy at regional, national and international levels. Consequently, building energy efficiency, energy efficient materials and technologies have become an area of significant research interest [9–11].

As a promising method to manage the intermittency and instability of energy supply, latent heat thermal energy storage technologies incorporating phase change materials (PCMs) have great potential for use in energy-efficient buildings [12–15]. Among various types of PCMs, organic PCMs are usually preferred as they pos-

* Corresponding author.
E-mail address: xingf@szu.edu.cn (F. Xing).

http://dx.doi.org/10.1016/j.apenergy.2016.10.072
0306-2619/

Nomenclature

PCM	phase change materials
HSB	hollow steel ball
PCM-HSB	macro-encapsulated PCM using HSB
PCM-HSB-c	PCM-HSB attached with a metal clamp (c)
PCM-HSBC-c	PCM-HSB-c concretes
ITZ	interfacial transition zone
RTD	rate of temperature decrease

sess competitive advantages in high energy storage capacity, good nucleation rate, small temperature variation from storage to reclamation, chemical stability, minimal segregation, little or no supercooling quality, and non-toxic properties [16,17].

In practice, leakage of PCMs during phase transition will happen if they are applied directly in building materials without being encapsulated. To address this issue, different techniques of incorporating PCMs into concrete have been studied, mainly including macro-encapsulation, micro-/nano-encapsulation and shape-stabilization. A large usage of micro-/nano-encapsulated PCM is of a higher cost and has an obvious adverse effect on the mechanical strength or thermal conductivity of the resulting building materials [18–20]. In contrast, macro-encapsulated PCM stored into comparatively larger form factors (tubes, spheres, pouches, panels, spheres, lightweight aggregates, etc.) can be applied into building elements without influencing the structural function of these elements in buildings [15,21–24]. Macro-encapsulated PCMs usually allows a higher content fraction of PCM to be incorporated into construction materials and also permit a higher encapsulation ratio of PCM [22,24,25]. Methods of macro-encapsulation have received great research attention in recent years because of their major advantages of easily low-cost production and direct use in concrete as aggregates or elements.

Different macro-encapsulation methods are chosen to suit different applications. For buildings, the macro-encapsulated PCM can be incorporated into the building wall as a thermal storage layer. Shi et al. [18] encapsulated PCM in a steel box and the box worked as a thermal shield layer which can be bonded externally or internally, or laminated within the building wall. Their test results showed that a PCM layer laminated within the wall gave the best temperature control performance and the peak indoor temperature was reduced by 4 °C. Lee et al. [26] sealed PCM with polymer pouches to prepare macro-encapsulated PCM. The sealed PCMs were also incorporated into building wall as a thermal shield layer. Additionally, macro-encapsulated PCM can be mixed with concrete for building applications. However, the main shortcomings of this macro-encapsulation method are associated with their low thermal conductivity and PCM leakage problems. To solve these problems, Alam et al. [27] coated the PCM while in its solid phase with a polymer layer by using the jar-milling technique.

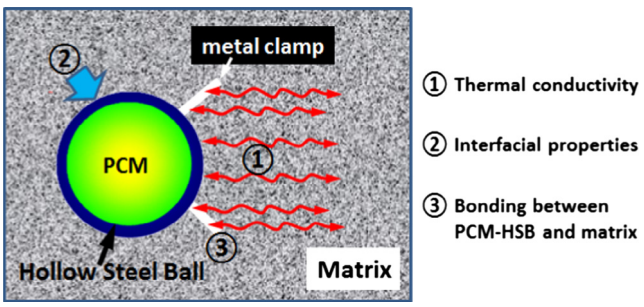

Fig. 1. Schematic drawing of a PCM-HSB-c in concrete matrix. ① metal clamp can improve thermal conductivity between PCM-HSB and matrix; ② metal clamp improves interfacial transition zone between PCM-HSB and matrix; ③ metal clamp can improve bonding between PCM-HSB and matrix.

An additional thin metal layer was then applied on top of the polymer coating to prevent leakage and maintain structural integrity when the PCM started melting.

Recently, a macro-encapsulated PCM using an innovative sealing technique for hollow steel balls (HSB) using washers and rivets was proposed by the authors [16]. Using HSB to carry PCM is a simple and functional method for PCM macro-encapsulation because the storage system can possess a much higher thermal conductivity and reliability compared to other macro-encapsulation methods. However, the general poor interfacial bonding and thermal conductivity between encapsulated PCM and matrix often reduces the compressive strength of the concrete and reduces the thermal function of the PCM. In order to solve these problems, in this research a metal clamp, which can improve both bonding and thermal conductivity, was innovatively attached to the PCM-HSB. Fig. 1 shows the innovation of this research with a schematic drawing of PCM-HSB-c in concrete matrix.

The compressive strengths of PCM-HSB-c concretes (PCM-HSBC-c) subject to different thermal cycles and elevated temperature conditions were studied to characterize the effect of the innovative PCM-HSB-c on interfacial and bonding properties. The thermal performances of PCM-HSBC-c panels were investigated using a self-designed environmental chamber to characterize the effect of the PCM-HSB-c on thermal conductivity.

2. Experimental work

2.1. Materials and sample preparation

PCM for this study is octadecane which is an organic paraffin manufactured by Sinopec Group, Henan Province, China. The physical properties of the PCM are displayed in Table 1.

The phase-change behavior of octadecane used in this study, including its latent heat, thawing and freezing temperatures, were measured by employing the test of differential scanning calorimetry (DSC, DSC-Q200, TA Instruments).

Fig. 2(a) shows an example of hollow steel ball (HSB) with a 22 mm nominal diameter which was used as the carrier for the PCM and coarse aggregate. There is a circular hole with a 2.7 mm diameter on each HSB, which allows the PCM to enter into it during the process of vacuum impregnation. The detail of HSB composited with PCM (PCM-HSB) preparation has been reported in the authors' previous study [16] and Table 2 lists the physical properties of the PCM-HSB.

The use of HSB as a carrier of PCM is considered to be an operative method for PCM macro-encapsulation, since the thermal reliability and conductivity of the energy storage system could be greatly improved. Each HSB is tightly secured by rivet and epoxy to prevent leakage of PCM so that the fire hazard of paraffin can

Table 1
Physical properties of the PCM (octadecane).

Density (g/cm^3)	Phase change temperature (°C)	Latent enthalpy of fusion (J/g)
0.78	27.1	249.7

a) HSB

b) Metal clamp

c) HSB attached with metal clamp (PCM-HSB-c)

Fig. 2. HSB and metal clamps.

be minimized. However, the surface of the HSB is very smooth, as shown in Fig. 2a, and results from the authors' previous study [16] showed that the poor mechanical bonding between the smooth HSB and mortar matrix has a negative effect on the compressive strength of PCM-HSB concrete. In order to enhance the mechanical interlocking at the aggregate-mortar interface, a kind of metal clamp (Fig. 2b) with rough edges was attached to each HSB. Fig. 2c shows a HSB attached with a metal clamp (HSB-c). The absorption mass ratio of PCM to the total mass of the HSB and the metal clamp is 61.7 wt% using a vacuum impregnation method, which matches previous studies [15,22].

Ordinary Portland cement, complying with the requirements of China National Standard GB 175-2007 (Common Portland Cement), was used for all concrete mixes investigated here. River sand, the fine aggregate used here, complied with ISO R679 (Methods of Testing Cements – Determinations of Strength). The fine aggregate has a density of 2600 kg/m^3 and a fineness modulus of 2.67. Crushed granite, the coarse aggregate, satisfied all requirements in BS EN 12620:2002 (Aggregates for concrete). Table 3 presents the detailed mix proportions of the control concrete and the PCM-HSB concretes. The masses of HSB and HSB-c were calculated based on their apparent densities in Table 2. For samples labelled "xx%-HSBC-c", the term "HSBC" is short for PCM-HSB concrete, "xx" denotes the volume as a percentage of the normal coarse aggregate that is replaced by PCM-HSB/PCM-HSB-c and "c" identifies HSB with metal clamps. This research studied the control concrete (Normal Concrete, NC) and the concretes with four different levels of PCM-HSB-c. 25%, 50%, 75% and 100% used to replace the normal coarse aggregate of the control concrete. In the compressive strength tests, a set of PCM-HSB concretes without the use of metal clamps was also studied for comparison.

The mixing procedures of the concrete with PCM-HSB-c were as follows. To begin with, all of the solid materials, except the PCM-HSB-c, were subjected to 1 min dry mix. Secondly, the dry mixture was added with water and superplasticiser then mixed for an additional 1 min. Lastly, PCM-HSB-c was added and mixing continued for another 1. It is worth noting that adding the PCM-HSB-c as the final component is done to minimize the possibility of damage to the PCM-HSB-c when mixing, because a prolonged mixing period may result in the detachment of metal clamps from the HSB. The mixing procedures of the concrete with PCM-HSB were same as that of PCM-HSB-c.

All the concrete samples were cured under standard conditions (RH $\geqslant$ 95%, 20 ± 2 °C) for 28 days before testing.

2.2. Test methods for PCM-HSBC-c properties

2.2.1. Compressive strength test

Based on Chinese standard GB/T 50081-2002 (Standard Test Method of Mechanical Properties on Ordinary Concrete), the compressive strength of concrete was determined with a loading rate of 0.5 MPa/s. The sample size was 100 mm L × 100 mm W × 100 mm H. For each mix, the reported 28-day compressive strength is the average strength of three samples. Then, multiplying it with a factor of 0.95 on the basis of the above standard, the strength was converted to the compressive strength of a 150-mm cube sample. The standard deviation of the compressive strength was not greater than 1.5 MPa.

2.2.2. Thermal performance test

The evaluation of thermal performance of the PCM-HSBC-c panels was carried out on samples with dimensions of 200 mm L × 200 mm W × 40 mm H using a self-designed environmental chamber (Fig. 3). The PCM-HSBC-c panels were used as the top element of small test rooms with an internal dimension of 200 mm L × 200 mm W × 200 mm H (see Fig. 3a). The remaining 5 panels were made of polystyrene foam, and the test rooms were sealed by silicon sealant to ensure void free application to the test room.

The environmental chamber, with internal dimension of 1000 mm L × 1000 mm W × 1000 mm H, was made of polystyrene foam panels. A heater and a portable air conditioner were installed

Table 2
Physical properties of PCM-HSB and PCM-HSB-c.

Inner diameter (mm)	Outer diameter (mm)	Hole diameter (mm)	Apparent density (kg/m^3)	
			PCM-HSB	PCM-HSB-c
20.6	22	2.7	1701	2645

Table 3
Mix proportion of concrete per cubic meter.

Kind	Bind (kg)	Water (kg)	Fine aggregate (kg)	Coarse aggregate (kg)	PCM-HSB-c (kg)	PCM-HSB (kg)	Admixture (kg)
NC (control)	400	140	787	1092	/	/	4
25%-HSBC-c	400	140	787	819	273	/	4
50%-HSBC-c	400	140	787	546	546	/	4
75%-HSBC-c	400	140	787	273	819	/	3.5
100%-HSBC-c	400	140	787	0	1022	/	3.5
25%-HSBC	400	140	787	819	/	175	4
50%-HSBC	400	140	787	546	/	350	4
75%-HSBC	400	140	787	273	/	525	3.5
100%-HSBC	400	140	787	0	/	701	3.5

Note: "xx%-HSBC", "xx" is the PCM-HSB/PCM-HSB-c volume replacement of normal coarse aggregate.

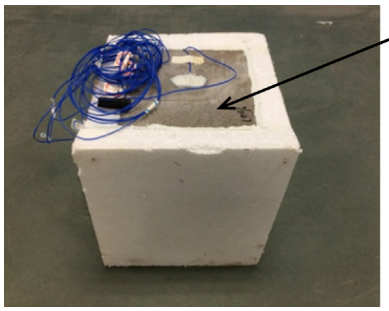

a) Room model with a concrete panel for thermal performance test

b) Self-designed environmental chamber with heater and air conditioner

Fig. 3. Sample and equipment for thermal performance.

to the chamber to control the working temperature of the chamber.

Five different room models (one with control concrete panel and the other four were concrete panels with different PCM-HSBC-c) were placed together beneath the bottom of the environmental chamber. Type K thermocouples (±0.3 °C resolution) were placed in each room model at three different positions (outer and inner surfaces of the concrete panel, and the center of the room) for temperature measurements. An additional thermocouple was placed at the center of the environmental chamber (the area to which the concrete panels were exposed) to measure the environmental temperature. The internal temperature of the chamber was raised and lowered by the heater and the portable air conditioner, respectively. To provide a uniform temperature to the test rooms, the hot or cold air was delivered from the top of the chamber. Consequently, the thermal responses of the PCM-HSBC-c panels under different temperature conditions can be measured.

All the test samples inside the environmental chamber were heated and cooled under the same conditions and duration. The top concrete panel was heated for a period of 8 h (started at 7:00) and was then cooled down by the air conditioner for another 8 h (ended at 23:00). Temperature measurements were recorded by a data-logger at a frequency of 60 s.

2.2.3. Strength reliability tests under thermal cycles

The strength reliability of PCM-HSBC-c was assessed by observing the changes in its compressive strength and interfacial transition zone (ITZ) after different thermal cycles of heating and cooling (30, 90 and 180 cycles). The thermal cycle test was carried out by placing the sample in a chamber with programmable

humidity and temperature (BE-TH-150H3, Dongguan Bell Experiment Equipment Co, Ltd., Dongguan, China). In this research, two PCM-HSB-c concretes (50%-HSBC-c and 75%-HSBC-c) were studied. In each 4-h thermal cycle, the chamber temperature heated from 10 °C to 60 °C in 20 min (at a rate of 2.5 °C/min) and maintained at 60 °C for 100 min, then it cooled to 10 °C in 20 min (at a rate of 2.5 °C/min) and maintained at 10 °C for 100 min. The chamber completed 6 thermal cycles in a day. For a thermal test of 30 cycles, 5 days were required. For 90 and 180 thermal cycles, 15 and 30 days were needed, respectively. Upon completion of the corresponding thermal cycles, compressive strength tests and microscopic studies were carried out to evaluate the effect of thermal cycles on the strength and microstructure of PCM-HSBC-c.

To investigate the influence of thermal cycles on the ITZ of PCM-HSBC-c, the microscopic studies on the ITZ between PCM-HSB-c and cement paste matrix was examined using Hitachi Su-70 FE-SEM (field emission-scanning electron microscope) with 1.0 kV accelerating voltage. A sample of 1–2 mm thick was taken from the ITZ of the PCM-HSBC-c. Extra care was taken to ensure the sample was not contaminated from leakage of the phase change materials (if any) during the thermal cycle test and that the cuts avoided the metal clamps. Gold was then deposited prior to observation. Fig. 4 shows the schematic position of ITZ to be examined and the observed area.

2.2.4. Elevated temperature test

The residual strength of concrete specimens (50%-HSBC-c and 75%-HSBC-c) after exposure to high temperature of 450 °C was investigated. A furnace (model no. JK-SX2-12-13N) with silicon carbide heating elements was used for the elevated temperature test. The internal dimension of the furnace is 300 mm × 500 mm × 200 mm (see Fig. 5). There were three samples for each test group, with the final reported strength the average of the three samples. According to the test method in the reference [28], the concrete cube samples after 28 days of standard curing were air-dried in the laboratory for 6 days and oven-dried at 105 °C for 24 h before the elevated temperature test. The specimens were heated at a rate of 10 °C/min up to 450 °C, and the temperature was maintained at 450 °C for 90 min. Thereafter, the samples were cooled naturally to an ambient temperature. Compressive strength test was executed to obtain the residual strengths of the concretes.

3. Results and discussions

3.1. Mechanical properties

3.1.1. Compressive strength

Fig. 6 compares the compressive strength of the concrete specimens with and without use of metal clamps. From this figure, it can be seen that the effect of the metal clamps on strength was not significant for the 25% PCM-HSB-c content in the concrete mixture. But the effect became significant when the PCM-HSB-c content increased to 50% or greater. As shown in Fig. 6, the strength of PCM-HSB-c concretes with metal clamps ranged between 41.2 and 28.1 MPa and the reduction of strength with regard to the control concrete ranged from 16 to 42% when the PCM-HSB-c content increased from 25 to 100%, respectively. However, the PCM-HSB-c concretes without metal clamps showed a reduction of 19–55% in compressive strength accordingly.

Fig. 7 shows the percentage reduction in the strength of PCM-HSB-c concretes with and without the use of metal clamps. The strength of PCM-HSB-c concretes with metal clamps was reduced about 20% when the PCM-HSB-c content was 75%, whereas the concrete without metal clamps showed a reduction of nearly 40%. When the PCM-HSB-c content increased to 100%, strength was reduced by reductions were 42% and 55% with and without metal clamps, respectively. It seems that the replacement level of PCM-HSB-c should not to exceed 75% in the mix, otherwise the concrete strength would be significantly reduced.

The results clearly demonstrated that the metal clamps can enhance the mechanical interlocking between the mortar and PCM-HSB-c aggregates and results in less reduction of compressive strength. With the aid of metal clamps, the PCM-HSBC-c is believed to have great potential for use as structural materials in buildings.

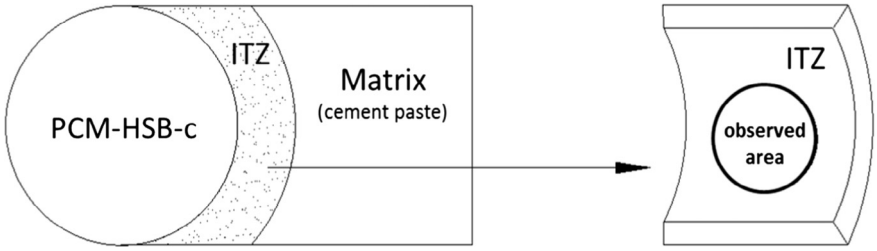

Fig. 4. Schematic position of sample for SEM study.

Fig. 5. Furnace and tested specimens.

3.1.2. Performance under thermal cycles

The effect of thermal cycling on the ITZ of the PCM-HSBC-c samples was studied in order to evaluate the strength reliability of PCM-HSBC-c. Fig. 8 shows the relationship between compressive strength and number of thermal cycles. It can be seen that after 90 thermal cycles the PCM-HSBC-c sample gave the highest compressive strength. After 90 thermal cycles, the strengths of 50%-HSBC and 75%-HSBC were increased by 14% and 22%, respectively. The main reason is due to the improvement in the ITZ between the cement paste and HSB during the thermal cycles.

The SEM images of the ITZ between the cement paste and HSB after different numbers of thermal cycles are shown in Fig. 9. An important difference between the micrographs obtained for samples before and after thermal cycling is in their apparent porosities. From Fig. 9a, it can be seen that the specimen without thermal cycling shows high porosity with large, interconnected pores in the ITZ. A high amount of coarse calcium hydroxide crystalline particles can also be observed in the ITZ. However, there is a significant difference in the microstructure of the ITZ when the specimen was subjected to 30 thermal cycles (Fig. 9b). Fig. 9b shows that the microstructure of the ITZ became less porous as more calcium silicate hydrate (C-S-H) gels are seen to fill up the pores. Escalante-Garcia [29] reported similar results, stating that the increased temperature during thermal cycling increased the rate of hydration of the clinker compounds, leading to denser microstructure and resulting in higher compressive strength. However, a few micro-cracks are still seen in the ITZ as shown in Fig. 9b. Fig. 9c shows the ITZ after 90 thermal cycles. From the figure, it can be seen that the microstructure after 90 thermal cycles was the most compact and homogeneously distributed structure with the lowest porosity compared. Fig. 9d shows the ITZ after exposure to 180 thermal cycles. The microstructure is very similar to those observed after 90 thermal cycles, but with more micro cracks observed in the ITZ. Previous studies have suggested that continual hydration at higher temperature for a long period of time has a deleterious effect on the mechanical properties [30].

To investigate the influence of thermal cycles on the internal pore structure of ITZ, the microstructures of concrete after exposure to 90 thermal cycles were observed at magnification of $\times$5000 and compared to that of concrete without thermal cycling (see Fig. 10). Fig. 10a shows that the microstructures of the ITZ without thermal cycling was of high porosity with lots of coarse $Ca(OH)_2$ particles and large pores. Apparently, the amount of calcium silicate hydrate (C-S-H) gel was not enough to fill up the pores and resulted in lower compressive strength. On the contrary, as shown in Fig. 10b, the microstructures of ITZ after exposed to 90 thermal cycles were of high density, more compact and more homogeneously distributed structure with lower porosity. The figure also shows that there were many small needle-like crystals of ettringite filling up the tiny pores in the ITZ. The SEM results demonstrate the effects of thermal cycling on the ITZ, and explain the compressive strength results of PCM-HSB-c concretes.

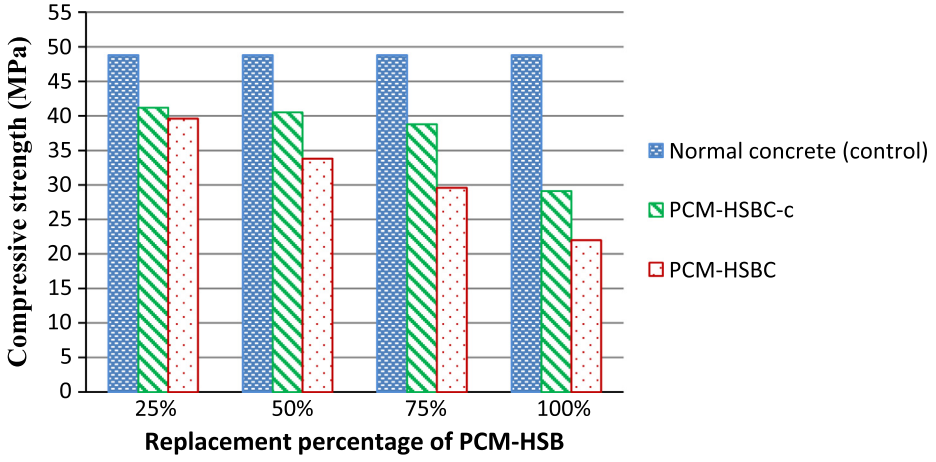

Fig. 6. Comparison of compressive strength between PCM-HSBC concretes with and without metal clamps.

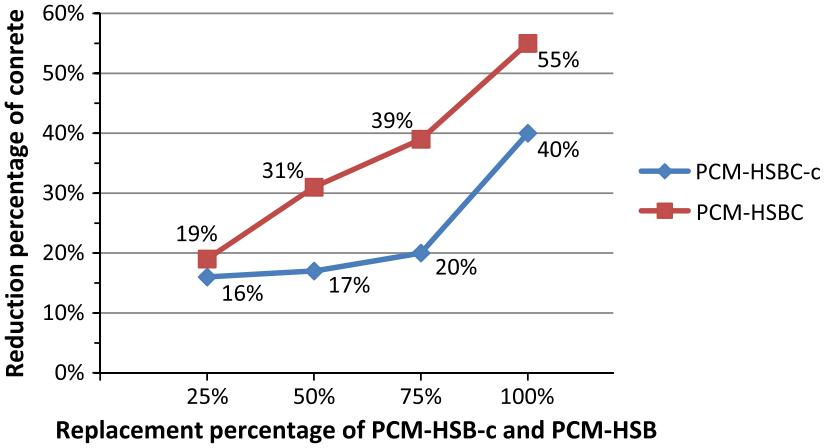

Fig. 7. Percentage reduction in strength of concretes with and without metal clamps.

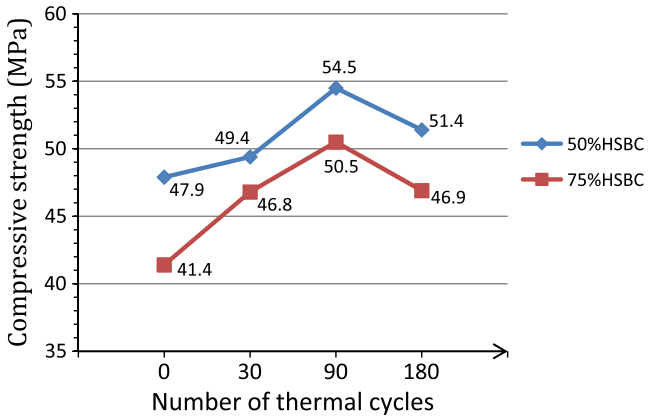

Fig. 8. Compressive strength of PCM-HSBC-c after exposed to different thermal cycles.

3.1.3. Performance at elevated temperature

Table 4 shows the residual compressive strengths of two PCM-HSB concretes after the elevated temperature test of 450 °C heat treatment for 90 min. It can be seen that for 50%-HSBC-c, the compressive strength decreased from 50.4 MPa to 47.9 MPa after the samples were exposed to elevated temperature. Similarly, the compressive strength of 75%-HSBC-c also decreased after the elevated temperature test. The reduction in compressive strength after heat treatment was less than 5% for both samples. Based on these test results, it is believed that the PCM-HSBC-c samples show strong fire resistance and are suitable for general building applications.

3.2. Thermal performance

3.2.1. Maximum temperature observed

The thermal performance of PCM-HSBC-c panels with different PCM-HSB-c contents was assessed by analysing the temperature changes at different positions when the environmental chamber was heating up and cooling down during the 16 h test period. The test results of maximum temperatures at the outer and inner surfaces of the concrete panel and at the center of the test room are displayed in Table 5. From Table 5, the control concrete panel showed not only the highest maximum temperature (43.8 °C) at the outer surface but also the greatest temperature difference (9.3 °C) between the outer surface of the panel and the center of the room. The indoor temperature for the room with PCM-HSBC-c panels was 1.2–2.0 °C lower than the control test room with a NC panel. These findings demonstrate that the PCM-HSBC-c panel possesses a high capacity of heat absorption and that the peak indoor room temperature can be lowered. From Table 5, the peak

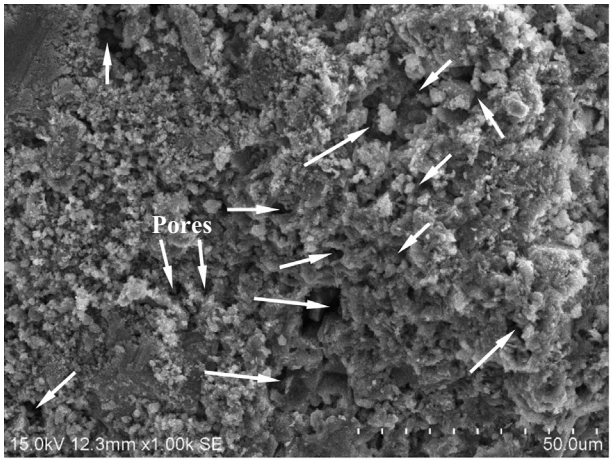

a) ITZ of sample of without thermal cycling

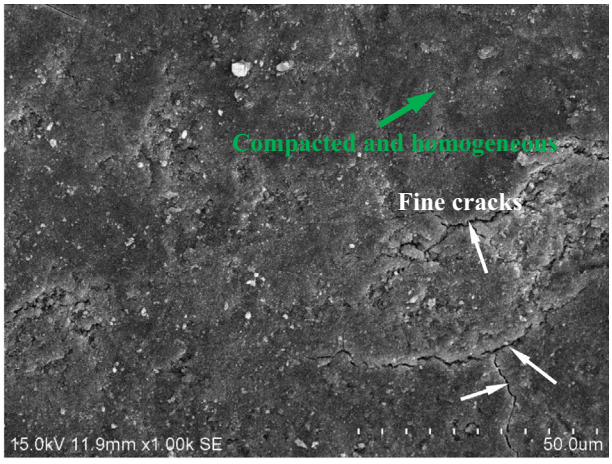

c) ITZ of sample exposed to 90 thermal cycles

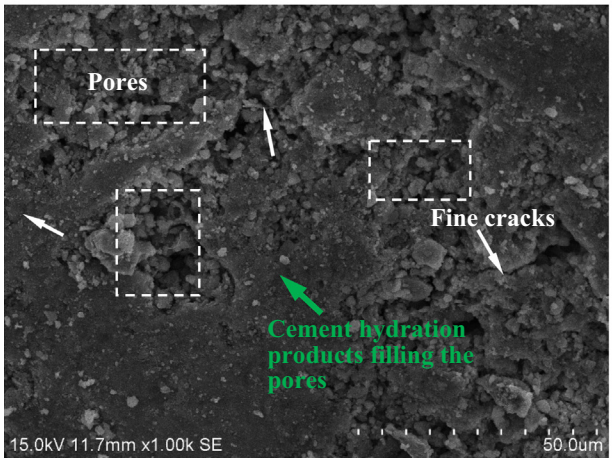

b) ITZ of sample exposed to 30 thermal cycles

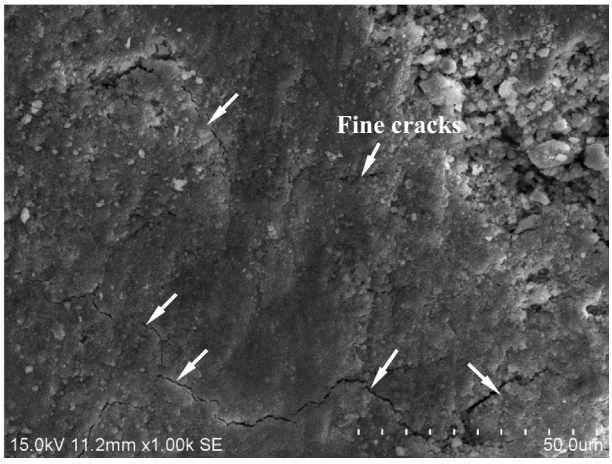

d) ITZ of sample exposed to 180 thermal cycles

Fig. 9. SEM images of specimens after exposed to different thermal cycles: (a) zero; (b) 30 cycles; (c) 90 cycles and (d) 180 cycles (×1000 magnification).

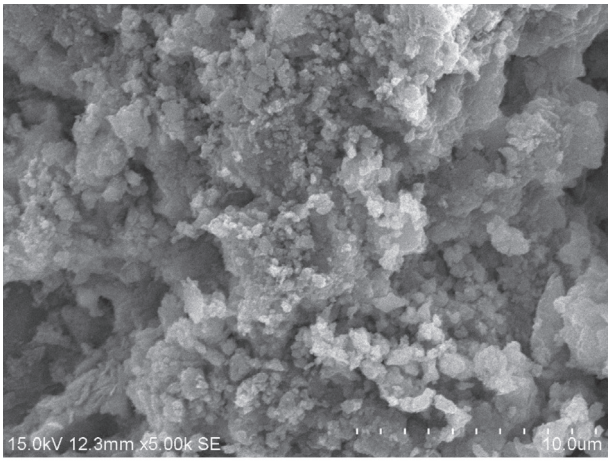

a) ITZ without thermal cycling

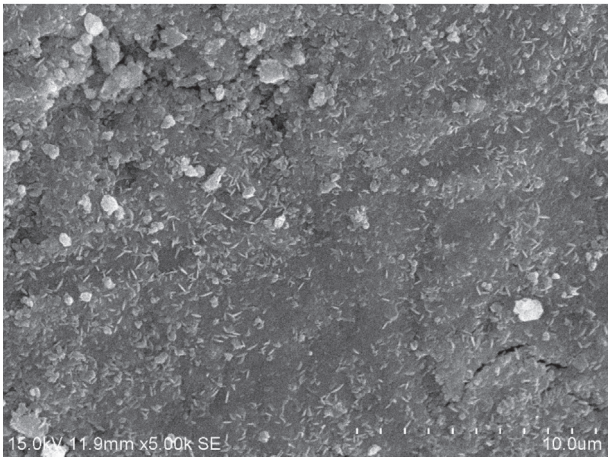

b) ITZ after exposed to 90 thermal cycles

Fig. 10. SEM images of specimens after exposed to (a) zero; (b) 90 thermal cycles (×5000 magnification).

Table 4
Residual compressive strength of PCM-HSBC-c after exposure to elevated temperature.

Specimen no.	Compressive strength before test (MPa)	Residual strength after test (MPa)
50%-HSBC-c	50.4	47.9
75%-HSBC-c	40.7	38.8

temperatures at the outer surfaces of all concrete panels with/without PCM-HSB were observed to occur at the same time (i.e., 15:00). Nevertheless, the peak temperature measured in the test rooms with PCM-HSB concrete panels was deferred by 2–7 min (IS) and 3–8 min (Indoor) compared with the time of peak temperatures in the control room model. The time delay was observed to increase with the rising proportion of PCM-HSB in the concrete panels.

3.2.2. Temperature observed at the outer and inner surfaces of PCM-HSBC-c panel

Figs. 11 and 12 show the temperature variations at two various positions of concrete panel made of different proportions of PCM-HSB-c. As can be seen from the figures, the temperature trends over time observed at the outer surface of the concrete panel (Fig. 11) are similar to those observed at the inner surface (Fig. 12) and their rates of temperature change are comparable. The main difference is the maximum temperatures measured. To discuss the effect of PCM-HSB-c contents on the temperature responses of concrete panel, both the heating and cooling processes during the thermal test were analysed.

At the beginning of the heating process (from 7:00 to 7:30), the rate of temperature increase (RTI) observed in all concrete panels were similar as phase change in the PCM-HSB-c samples was yet to take place. After 1 h (at 8:00), the PCM-HSB-c in the concrete panel started to take effect and absorb heat, resulting in a decrease of RTI in PCM-HSBC-c panels. This reduction became significant when the PCM-HSB-c content increased, whereas the RTI observed in NC panel remained steady up to 11:00, then gradually slowing until the end of the heating process. The NC panel recorded the highest temperature values at all times in the heating process, as shown in Figs. 11 and 12. After 1.5 h (at 8:30), the PCM-HSB-c started to take significant effect and the RTI reduced significantly. The temperature curves for concrete panels with PCM-HSB-c content of 50% or more became nearly flat as shown in Figs. 11 and 12. The plateau in the figures is described as the phase change zone, where the PCM transition between the solid and liquid states and they continued to melt until no solid remained. In general, the length of the phase change zone observed as it is at the inner surface is longer than that observed at outer surface. It is worthy to note that the length of the phase change zone increased with an increased content of PCM-HSB-c in the panel. In case of the 100%-HSBC-c panel specimen, the temperatures at the outer and inner surfaces of the panel remained nearly constant between 9:00 and 12:00. The temperatures measured at the inner and outer surfaces during this period were in the range of 29–30.5 °C and 27–28 °C, respectively. This implies that concrete with higher PCM-HSB-c content would have a greater ability to maintain the indoor room temperature for a longer period of time. When the phase change effect of PCM-HSB-c was exhausted (as all PCM melted), the figures show that the RTI of PCM-HSBC-c panels began to increase, and even at a faster rate at the end of the heating stage compared to the NC concrete panel. The reason is due to the excellent thermal conductivity of the steel balls and metal clamps that showed a quick response to temperature changes.

After the heating stage was completed, cooling was started at 15:00. It can be seen from Figs. 11 and 12 that the temperature observed at all concrete panels dropped significantly within the first cooling hour. The rate of temperature decrease (RTD) observed in all concrete panels was similar as the phase transition in the PCM-HSB-c samples was yet to take place. At 16:00, after 1 h of cooling, the PCM-HSB-c in the concrete panels started to take effect and released heat which slowed down the RTD in PCM-HSBC-c panels. Again, this effect is more significant when the PCM-HSB-c content is increased, whereas the RTD observed in NC panel remained steady up to 18:00. The NC panel gave the lowest temperature values at all times in the cooling process, as shown in Figs. 11 and 12. After 1 h cooling time (at 16:00), the PCM-HSB started to take significant effect and the RTD was significantly reduced, the temperature curves for concrete panels with PCM-HSB-c content of 50% or more became nearly flat as shown in Figs. 11 and 12. Similarly with the heating cycle, this plateau in the figures is described as the phase change zone where the PCM transitions between the liquid and solid states and continued to solidify until completely solid. In general, the length of the phase change zone observed at the inner surface is similar to that observed at the outer surface. Likewise, the length of the phase change zone increased with the increase of PCM-HSB content in the panel. In case of the 100%-HSBC panel specimen, the temperature at outer and inner surfaces of the panel remained nearly constant between 16:00 and 19:00. The temperatures measured at

Table 5
Thermal properties of room model using different PCM-HSBC-c panels.

Sample no.	The highest temperature				Time of the peak temperature		
	OS	IS	Indoor	Difference between Indoor and OS	OS	IS	Indoor
NC (control)	43.8	41.7	34.5	9.3	15:00	15:02 (+0.02)	15:03 (+0.03)
25%-HSBC-c	41.6	39.5	33.3	8.3	15:00	15:03 (+0.03)	15:04 (+0.04)
50%-HSBC-c	40.9	39.1	32.7	8.2	15:00	15:04 (+0.04)	15:05 (+0.05)
75%-HSBC-c	40.6	39.1	32.7	7.9	15:00	15:06 (+0.06)	15:07 (+0.07)
100%-HSBC-c	39.9	37.9	32.5	7.4	15:00	15:07 (+0.07)	15:08 (+0.08)

Note: OS = Outer surface; IS = Inner surface; Indoor refers the temperature at the center of the room.

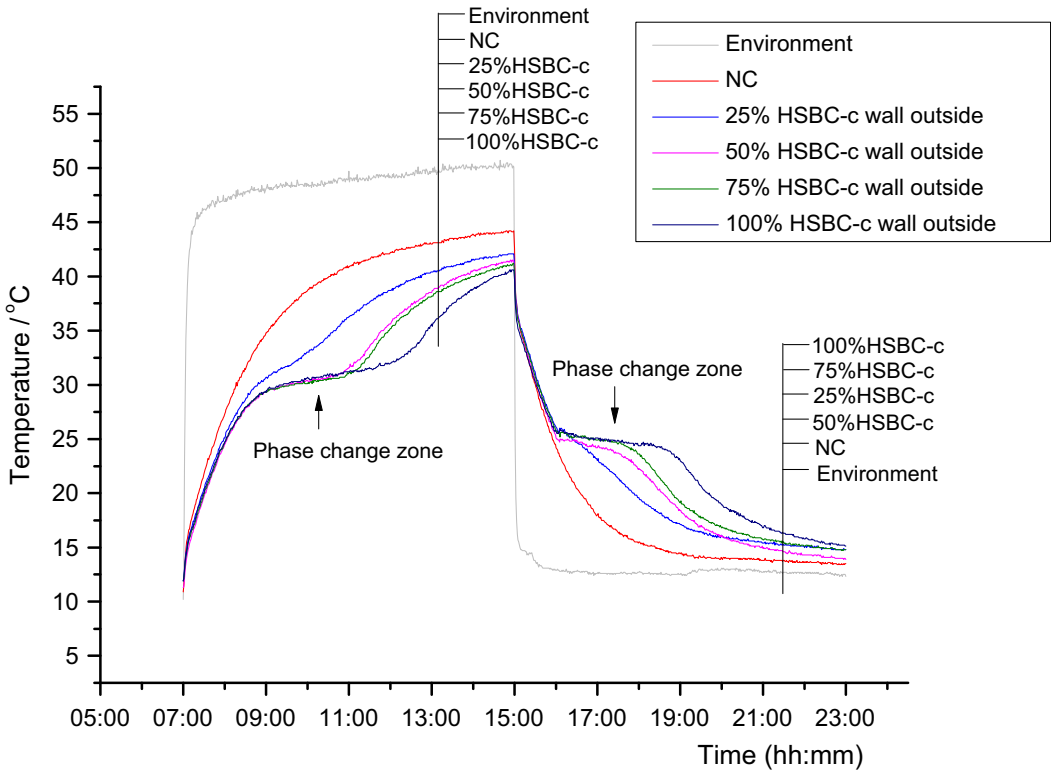

Fig. 11. Temperature curves of test room models with 5 different PCM-HSBC-c panels (measured from outer surface of the panel).

inner and outer surfaces during this period were in the range of 26.5–27.0 °C and 23.5–25 °C, respectively. This further demonstrates that concrete with higher PCM-HSB content would have a greater ability to maintain the indoor room temperature for a longer period of time. When the phase change effect of the PCM-HSB disappeared (as all PCM solidified), the figures show that the RTD of PCM-HSBC-c panels began to increase. Again, the temperature increased in the PCM-HSB-cat an even faster rate at the end of the heating stage compared to the control concrete panel. This is due to the excellent thermal conductivity of the steel balls and metal clamps, as mentioned earlier.

3.2.3. Indoor temperature observed at room models made of PCM-HSBC-c panel

The variation curves for indoor temperature of the room models using different concrete panels are shown in Fig. 13. In the beginning of heating process (from 7:00 to 7:30), the RTI observed in all room models were similar, because the PCM-HSB-c was yet to function when below its phase change temperature. When the heating time increased to 1 h (at 8:00), the room models using PCM-HSBC-c panels were observed to have lower indoor RTI during the heating process compared to the control room model. The effect became more significant when the PCM-HSB-c content increased, whereas the RTI observed in control room model remained steady up to 11:00 before gradually slowing. This phenomenon can be explained by the fact that part of the heating load could be taken by the melting of PCM in the PCM-HSB-c. After heating for 1.5 h (at 8:30), the PCM-HSB-c started to take effect and the RTI significantly reduced. The temperature curves for the concrete panels with PCM-HSB-c content of 50% or more became nearly flat as shown in Fig. 13. In general, the length of the phase change zone could be prolonged and the indoor temperature could be decreased by increasing the PCM-HSB-c content in the concrete panel. From 8:30 to 12:30, the difference in indoor temperatures between the control concrete room and the rooms with PCM-HSB-c panels became much more significant. The temperature measured inside the NC and 100%-HSBC-c rooms during this 4 h period were in the range of 28–34 °C and 26–27.5 °C, respectively. The temperature difference observed between these two rooms reached up to 6.5 °C. The peak indoor temperatures were 35.5 °C and 32–33.5 °C for the control room and the PCM-HSBC-c rooms, respectively. The rooms with 50%-HSBC-c and 75%-HSBC-c concrete panels have very similar temperature curves and have lower indoor temperatures than that of the room with concrete panel made of 25%-HSBC-c. However, the room with 100%-HSBC-c concrete panel showed the

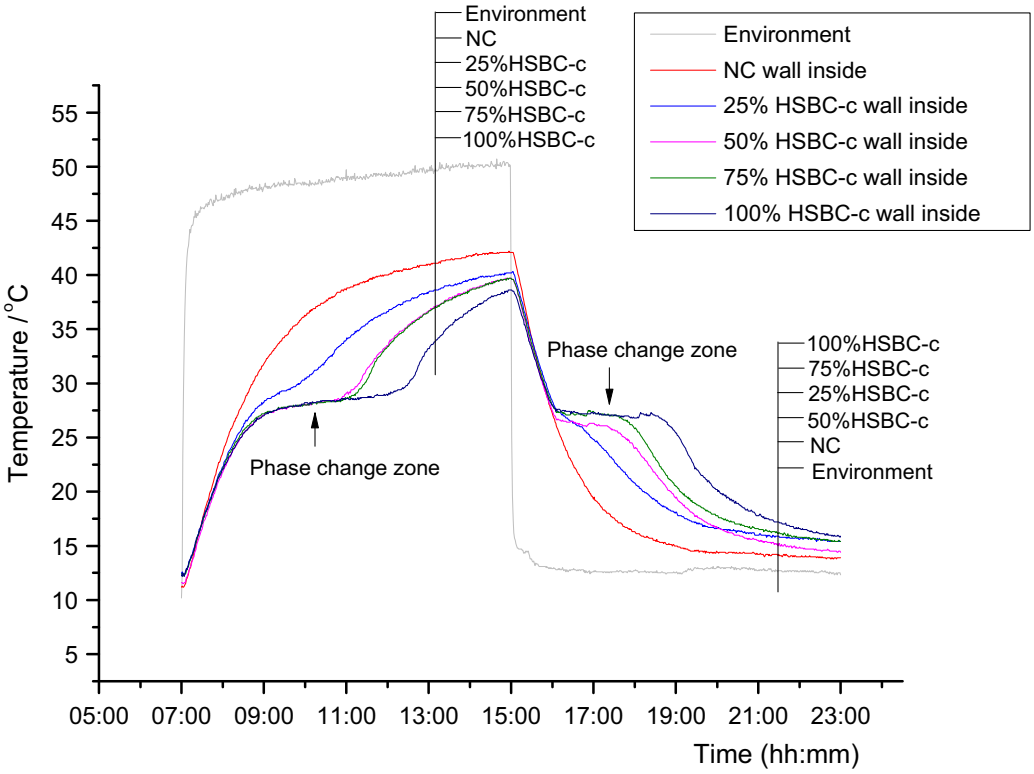

Fig. 12. Temperature curves of test room models with 5 different PCM-HSBC-c panels (measured from inner surface of the panel).

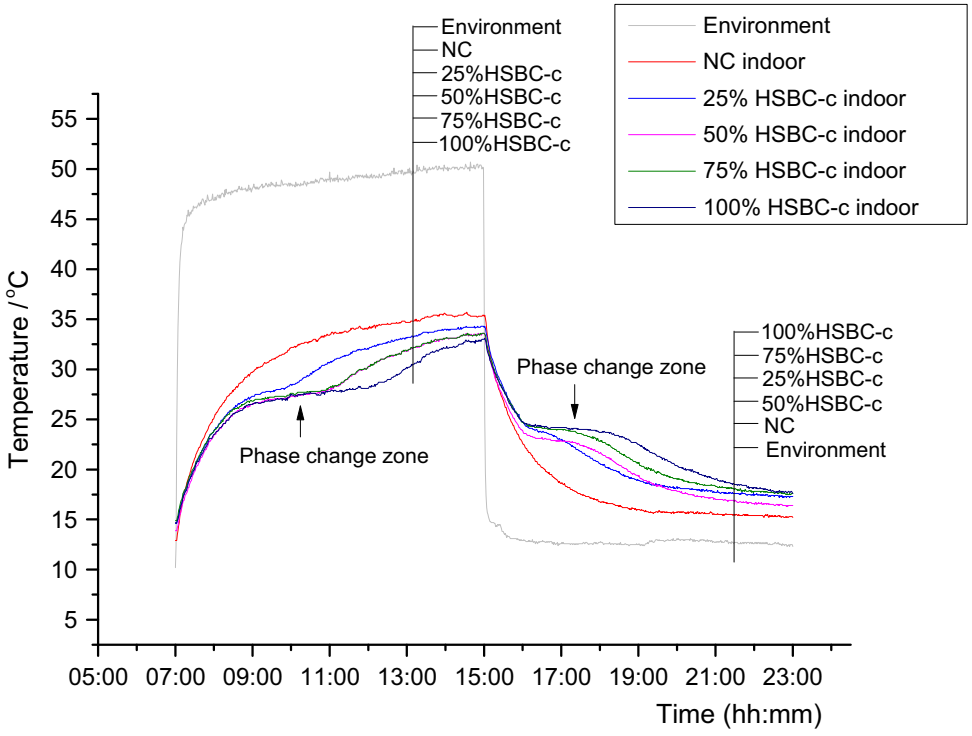

Fig. 13. Indoor temperature curves of test room models with 5 different PCM-HSB-c panels.

lowest indoor peak temperature. These results show that concrete with higher PCM-HSB-c content have a greater ability to maintain a relatively low indoor room temperature for a longer period of time. Similar to what observed in the surfaces of PCM-HSB-c panels, the RTI of PCM-HSBC-c panels began to increase, and even at a faster rate at the end of the heating stage compared to the NC concrete panel.

After stopping heating, the room models were all cooled down close to the environmental temperature of approximately 13 °C. As indicated in Fig. 13, the indoor temperature dropped significantly

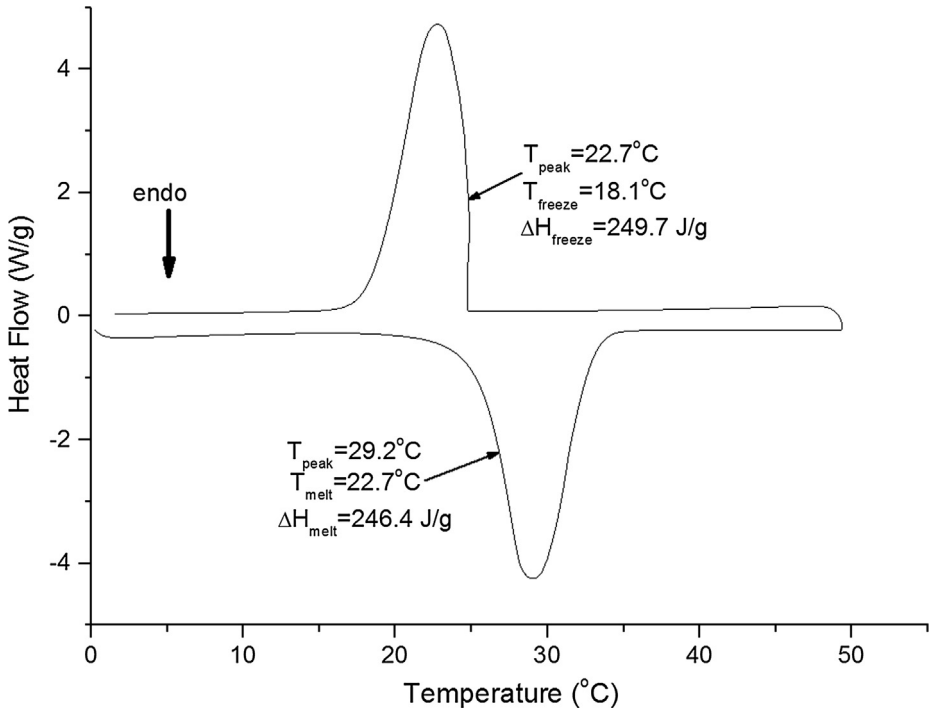

Fig. 14. Curves of DSC test for the PCM (octadecane) used in this study.

within the first hour of cooling. The RTD observed in all room models was similar as the PCM-HSB-c was yet to take place. At 16:00, the PCM-HSB-c in the concrete panel started to take effect and release latent heat which slows down the RTD. This effect is increased when the PCM-HSB-c content is increased, whereas the RTD observed in the control room remained steady up to 18:00. The control room gave the lowest indoor temperature values at all times during the cooling process, as shown in Fig. 13. After 1 h of cooling (at 16:00), the temperature curves for concrete panels with PCM-HSB-c content of 50% or more became nearly flat and the length of phase change zone was prolonged with an increase in PCM-HSB-c content in the concrete panel. It can be deduced that PCM in PCM-HSB-c began to solidify and release heat, which reduced the cooling rate and maintained the indoor temperature. This phenomenon became obvious after 16:00. The 100%-HSBC room model showed a steady indoor temperature for a period of 3.5 and 3 h during the heating and cooling processes, respectively. As shown in Fig. 13, the rooms with PCM-HSB-c had higher indoor temperatures than that of the control room model during the time from 16:00 to the end of cooling stage, and the effect became more significant when the content of PCM-HSB-c increased in the panel. The temperature measured inside the NC and 100%-HSBC-c rooms during the 3 h period from 16:00 to 19:00 were in the range of 14–23.5 °C and 21.5–23 °C, respectively. The difference in indoor temperature s between these two rooms was up to 9 °C. This phenomenon proved that concrete panel with PCM–HSB-c is effective in limiting the fluctuations of indoor temperatures. Therefore, the PCM–HSB-c concrete has a great potential in decreasing energy consumption by restricting temperature fluctuations and shifting heating or cooling load away from the peak period. For this reason, PCM–HSB-c is suitable for applications in building materials. Higher content fractions of PCM–HSB-c are recommended, due to a shorter phase change zone observed for the 25%-HSBC-c specimen.

3.2.4. Energy storage capacity of PCM-HSB-c

Fig. 14 shows the octadecane paraffin's DSC curve, showing the phase change temperature of the paraffin ranged from 24 to 33 °C for the thawing stage and 25–17 °C for the freezing stage. Furthermore, the latent heat and peak temperature of thawing is 246.4 J/g and 29.2 °C for the melting process of the paraffin. Similarly, the enthalpy and solidification temperature for the freezing process is 249.7 J/g and 22.7 °C, respectively. Therefore, the average latent heat of the paraffin is around 248.1 J/g. The influence of the heating/cooling rates on DSC test results was carried out by Kheradmand et al. [31]. That study showed that even if the total thermograms differences under different heating/cooling rate can become lesser with the rate decreasing; but the accumulated latent heat is nearly constant irrespective of the rate of heating or cooling. The encapsulation ratio of PCM mass to the total mass of the HSB and metal clamp is 61.7 wt% based on a vacuum impregnation encapsulation test. Therefore, the latent heat that PCM-HSB-c can acquire is approximately 153.1 J/g (248.1 × 61.7% = 153.1). From values reported in literature [22,25,32,33], it is shown that the general latent heat range from 15 J/g to 150 J/g. In this study, the latent heat of PCM-HSB-c can be considered to rank highly among values from literature. Due to the larger latent heat of PCM, the higher energy storage capacity the PCM is, therefore, the concretes with different contents of PCM-HSB-c, which were developed in this study. As a result, PCM-HSB-c have huge potential for thermal energy storage in different types of buildings.

4. Conclusions

In this study, an innovative method of macro-encapsulation of PCM was developed using hollow steel balls (HSB) attached with metal clamps to improve mechanical bonding to the mortar matrix. The mechanical and thermal performance of HSBC-c concrete was investigated. Based on the above discussions, the following conclusions can be drawn:

(1) The metal clamps enhanced the mechanical interlocking between the mortar and HSB aggregates, resulting in less compressive strength reduction compared to samples without clamps. With the aid of metal clamps, the PCM-HSBC-c is

believed to have great potential for use as structural materials in buildings.

(2) The strengths of PCM-HSBC-c increased with an increasing number of thermal cycles. After 90 thermal cycles, the strengths of 50%-HSBC-c and 75%-HSBC-c were increased by 14% and 22%, respectively. The main reason is due to the improvement in ITZ between the cement paste and HSB during the thermal cycles.

(3) The increased temperature during thermal cycles increased the degree of hydration of the cement in PCM-HSB-c concrete, leading to a denser microstructure and higher compressive strength. The SEM results showed that after 90 thermal cycles the microstructure was the most compact and homogeneously distributed structure with the lowest porosity, thus giving the peak compressive strength.

(4) In the up to 450 °C elevated temperature test, the strengths of 50%-HSBC and 75%-HSBC reduced by less than 5%. It indicated the PCM-HSB-c concretes have comparative good fire resisting performance and have potential applications as energy efficiency building materials.

(5) According to the thermal performance results with the use of a self-designed environmental chamber, the PCM–HSB-c concrete panel is able to reduce the indoor temperature fluctuation and decrease the loads of heating and cooling significantly. The PCM–HSB-c concrete panel can also shift the thermal loads away from the times of peak energy demand. An increase in PCM-HSB-c contents further improved the thermal performance and lengthened the phase change zone. In consideration of the mechanical properties, thermal performance and other aspects of economic factors, 50% and 75% PCM-HSB-c replacement levels are recommended in producing structural-functional integrated concrete.

(6) Due to the high energy storage capacity of the PCM-HSB-c, the concretes with different content fractions of PCM-HSB-c have great potential for thermal energy storage in different types of buildings.

Acknowledgments

The work described in this paper was fully supported by grants from Natural Science Foundation of China (51372155), Natural Science Foundation of China (51678367) and Australian Research Council Discovery Project (G1500225).

References

[1] da Cunha JP, Eames P. Thermal energy storage for low and medium temperature applications using phase change materials – a review. Appl Energy 2016;177:227–38.
[2] Karaipekli A, Sarı A. Development and thermal performance of pumice/organic PCM/gypsum composite plasters for thermal energy storage in buildings. Sol Energy Mater Sol Cells 2016;149:19–28.
[3] International energy outlook, vol. 1. Energy Information Administration; 2016.
[4] Annual energy outlook 2015: with projections to 2040. EIA (Energy Information Administration); 2015.
[5] Gruber M, Trüschel A, Dalenbäck J-O. Energy efficient climate control in office buildings without giving up implementability. Appl Energy 2015;154:934–43.
[6] Ionescu C, Baracu T, Vlad G-E, Necula H, Badea A. The historical evolution of the energy efficient buildings. Renew Sustain Energy Rev 2015;49:243–53.
[7] Liu Z, Zhang L, Gong G, Li H, Tang G. Review of solar thermoelectric cooling technologies for use in zero energy buildings. Energy Build 2015;102:207–16.
[8] Bryant T, Thomas S, Dean B, Lyons L, Morgado D, Je KH, et al. IEA energy efficiency market report; 2015.
[9] Tyagi V, Pandey A, Buddhi D, Kothari R. Thermal performance assessment of encapsulated PCM based thermal management system to reduce peak energy demand in buildings. Energy Build 2016;117:44–52.
[10] Virgone J, Giroux-Julien S. Modeling of an active facade containing Phase Change Materials. In: Conférence CLIMAMED, Juan-les-Pins, septembre.
[11] Agyenim F. The use of enhanced heat transfer phase change materials (PCM) to improve the coefficient of performance (COP) of solar powered LiBr/H_2O absorption cooling systems. Renew Energy 2016;87:229–39.
[12] Yang J, Yang L, Xu C, Du X. Experimental study on enhancement of thermal energy storage with phase-change material. Appl Energy 2016;169:164–76.
[13] Iten M, Liu S, Shukla A. A review on the air-PCM-TES application for free cooling and heating in the buildings. Renew Sustain Energy Rev 2016;61:175–86.
[14] Mi X, Liu R, Cui H, Memon SA, Xing F, Lo Y. Energy and economic analysis of building integrated with PCM in different cities of China. Appl Energy 2016;175:324–36.
[15] Memon SA, Cui H, Lo TY, Li Q. Development of structural–functional integrated concrete with macro-encapsulated PCM for thermal energy storage. Appl Energy 2015;150:245–57.
[16] Dong Z, Cui H, Tang W, Chen D, Wen H. Development of hollow steel ball macro-encapsulated PCM for thermal energy storage concrete. Materials 2016;9:59.
[17] Souayfane F, Fardoun F, Biwole P-H. Phase change materials (PCM) for cooling applications in buildings: a review. Energy Build 2016;129:396–431.
[18] Yu S, Wang X, Wu D. Microencapsulation of n-octadecane phase change material with calcium carbonate shell for enhancement of thermal conductivity and serving durability: synthesis, microstructure, and performance evaluation. Appl Energy 2014;114:632–43.
[19] Sarı A, Alkan C, Bilgin C. Micro/nano encapsulation of some paraffin eutectic mixtures with poly(methyl methacrylate) shell: preparation, characterization and latent heat thermal energy storage properties. Appl Energy 2014;136:217–27.
[20] Jiang X, Luo R, Peng F, Fang Y, Akiyama T, Wang S. Synthesis, characterization and thermal properties of paraffin microcapsules modified with nano-Al_2O_3. Appl Energy 2015;137:731–7.
[21] Jin X, Medina MA, Zhang X. On the importance of the location of PCMs in building walls for enhanced thermal performance. Appl Energy 2013;106:72–8.
[22] Cui H, Memon SA, Liu R. Development, mechanical properties and numerical simulation of macro encapsulated thermal energy storage concrete. Energy Build 2015;96:162–74.
[23] Akeiber H, Nejat P, Majid MZA, Wahid MA, Jomehzadeh F, Famileh IZ, et al. A review on phase change material (PCM) for sustainable passive cooling in building envelopes. Renew Sustain Energy Rev 2016;60:1470–97.
[24] Kastiukas G, Zhou X, Castro-Gomes J. Development and optimisation of phase change material-impregnated lightweight aggregates for geopolymer composites made from aluminosilicate rich mud and milled glass powder. Constr Build Mater 2016;110:201–10.
[25] Memon SA, Cui HZ, Zhang H, Xing F. Utilization of macro encapsulated phase change materials for the development of thermal energy storage and structural lightweight aggregate concrete. Appl Energy 2015;139:43–55.
[26] Lee KO, Medina MA, Raith E, Sun X. Assessing the integration of a thin phase change material (PCM) layer in a residential building wall for heat transfer reduction and management. Appl Energy 2015;137:699–706.
[27] Alam TE, Dhau JS, Goswami DY, Stefanakos E. Macroencapsulation and characterization of phase change materials for latent heat thermal energy storage systems. Appl Energy 2015;154:92–101.
[28] Arioz O. Effects of elevated temperatures on properties of concrete. Fire Saf J 2007;42:516–22.
[29] Escalante-García JI, Sharp JH. The microstructure and mechanical properties of blended cements hydrated at various temperatures. Cem Concr Res 2001;31:695–702.
[30] Komendant J, Nicolayeff V, Polivka M, Pirtz D. Effect of temperature, stress level, and age at loading on creep of sealed concrete. Spec Publ 1978;55:55–82.
[31] Kheradmand M, Azenha M, Aguiar JLBD, Krakowiak KJ. Thermal behavior of cement based plastering mortar containing hybrid microencapsulated phase change materials. Energy Build 2014;84:526–36.
[32] Memon S, Liao W, Yang S, Cui H, Shah S. Development of composite PCMs by incorporation of paraffin into various building materials. Materials 2015;8:499.
[33] Cui H, Liao W, Memon S, Dong B, Tang W. Thermophysical and mechanical properties of hardened cement paste with microencapsulated phase change materials for energy storage. Materials 2014;7:8070–87.